

Electronic Supplementary Information

Stabilizing Cu⁰-Cu⁺ sites by Pb-doping for highly efficient CO₂ electroreduction to C₂ products

Xiaodong Ma,^{a,b} Xinning Song,^{a,b} Libing Zhang,^{a,b} Limin Wu,^{a,b} Jiaqi Feng,^{a,b} Shunhan Jia,^{a,b} Xingxing Tan,^{a,b} Liang Xu,^{a,b} Xiaofu Sun,^{a,b}* and Buxing Han,^{a,b,c}*

a. Beijing National Laboratory for Molecular Sciences, Key Laboratory of Colloid and Interface and Thermodynamics, Center for Carbon Neutral Chemistry, Institute of Chemistry, Chinese Academy of Sciences, Beijing 100190, P. R. China.

Email: sunxiaofu@iccas.ac.cn; hanbx@iccas.ac.cn

b. School of Chemical Sciences, University of Chinese Academy of Sciences; Beijing 100049, P. R. China.

c. Shanghai Key Laboratory of Green Chemistry and Chemical Processes, School of Chemistry and Molecular Engineering, East China Normal University, Shanghai 200062, P. R. China.

Supporting Methods

Chemicals and materials.

Copper sulfate pentahydrate ($\text{CuSO}_4 \cdot 5\text{H}_2\text{O}$, 99.0%), oleic acid (OA, AR), ethanol (99%), D-(+)-glucose (99%), acetone (99%), sodium hydroxide (NaOH, 99%), potassium hydroxide (KOH, GR, 85%), lead acetate trihydrate ($\text{Pb}(\text{CH}_3\text{COO})_2 \cdot 3\text{H}_2\text{O}$, 99.0%), Nafion D-521 (5% wt%), isopropanol (99%), D_2O , Nafion N-117 membrane, and GDE hydrophobic carbon paper were purchased from Alfa Aesar China Company. CO_2 (99.999%) was provided by Beijing Analytical Instrument Company. Deionized water was used in all experiments.

Synthesis of Cu_2O : In a typical procedure, 1 mmol $\text{CuSO}_4 \cdot 5\text{H}_2\text{O}$ was dissolved in 15 mL of deionized water in a glass flask and heated to 80 °C. Then 2 mL of OA and 5 mL of ethanol were added to the solution with maintained stirring for 30 min at 80°C. After that, 5 mL of 1M NaOH aqueous solution was added to the flask and kept stirring for 10 min at 80°C. Finally, 5 mL of 2M glucose solution was added into the flask and kept the reaction at 80°C for 3 hours. The reddish brown solid products were collected and washed with cyclohexane and water, and then dried under vacuum at 60 °C for 12 h to obtain Cu_2O .

Synthesis of $\text{Pb}/\text{Cu}_2\text{O}$ -x (x = Mass fraction of Pb): In a typical procedure, 50 mmol $\text{Pb}(\text{CH}_3\text{COO})_2 \cdot 3\text{H}_2\text{O}$ was dissolved in 50 mL of deionized water in a glass flask. After that, 100 mg of the synthesized Cu_2O powder was added into the lead acetate solution and evenly dispersed. Then, the mixture was stirred under the condition of isolating air and avoiding light. After stirring, the reddish brown solid products were collected and washed with water, and then dried under vacuum at 60 °C for 12 h to obtain $\text{Pb}/\text{Cu}_2\text{O}$ -x. x is the mass fraction of Pb measured by inductively coupled plasma optical emission spectroscopy (ICP-OES) and X-ray photoelectron spectroscopy (XPS). By adjusting the stirring time of Cu_2O in lead acetate solution, $\text{Pb}/\text{Cu}_2\text{O}$ -x with different Pb doping contents can be obtained. When the stirring time was 12h, 24h, 48h, and 150h, the synthesized $\text{Pb}/\text{Cu}_2\text{O}$ -x was $\text{Pb}/\text{Cu}_2\text{O}$ -1.2%, $\text{Pb}/\text{Cu}_2\text{O}$ -2.1%, $\text{Pb}/\text{Cu}_2\text{O}$ -3.4%, and $\text{Pb}/\text{Cu}_2\text{O}$ -6.2%, respectively.

Preparation of e- $\text{Pb}/\text{Cu}_2\text{O}$ -x GDE (x = Mass fraction of Pb): 10 mg of the synthesized $\text{Pb}/\text{Cu}_2\text{O}$ -x material was added in 1 mL of acetone and evenly dispersed. Then 400 μL dispersion liquid was sprayed on 2.7 cm \times 2 cm gas diffusion electrode hydrophobic carbon paper.

Subsequently, 100 μL 10%wt% Nafion D-521 isopropanol solution was sprayed on the GDE. After electrochemical activation of GDE in 3M KOH solution at -1.0 V vs. RHE for 3 min, e-Pb/Cu₂O-x loaded GDE was obtained.

Catalysts Characterization.

The ratio of Cu and Pb elements in the e-Pb/Cu₂O-x were determined by inductively coupled plasma optical emission spectroscopy (ICP-OES, Vista-MPX). The morphologies and sizes of e-Pb/Cu₂O-x were observed on HITACHI S-4800 scanning electron microscope (SEM) and a JEOL JEM-2100F high-resolution transmission electron microscopy (HR-TEM), and element distribution of e-Pb/Cu₂O-x were observed on energy dispersive spectrometer (EDS). X-ray diffraction (XRD) patterns of e-Pb/Cu₂O-x were characterized by using Rigaku Model D/MAX2500. XPS spectra of e-Pb/Cu₂O-x were collected on the Thermo Scientific ESCA Lab 250Xi using 200 W monochromatic Al K α radiation and calibrated against C 1s at 284.8 eV. The Cu K-edge and Pb L-edge XAS were collected at the 1W1B and 4B9A beamline of Beijing Synchrotron Radiation Facility.

Electrochemical CO₂RR over e-Pb/Cu₂O-x.

All the electrochemical experiments were performed on the CHI 660E electrochemical workstation. The electrolysis experiments were conducted at room temperature in the flow cell. The e-Pb/Cu₂O-x loaded GDE was used as the cathode of the electrochemical experiment, the Ag/AgCl electrode was used as the reference electrode, and the foam Ni was used as the anode in the electrochemical experiment. Anion exchange membrane (FumasepFAA-3-PK-130) was placed between the cathodic and anodic chambers. 3 M KOH aqueous solution was used as the electrolyte. In each experiment, the amount of cathode electrolyte used is 10 mL, and the amount of anode electrolyte is 30 mL. During the reaction, the electrolyte is circulated at a speed of 40 mL min⁻¹ through a peristaltic pump. A stable CO₂ gas flow is continuously introduced into GDE, and the flow rate of CO₂ gas flow is 40 sccm.

Products quantitative analysis:

The gaseous product was analyzed in gas chromatography (GC, HP 4890D), and the liquid product was analyzed by ¹H NMR (Bruker Avance III 400 HD spectrometer). In NMR spectra, the

D₂O as deuterium reagent, the sodium 2, 2-dimethyl-2-silapentane-5-sulfonate (DSS) and phenol were used as the internal standard of product. 400 μL catholyte was mixed with 100 μL 6 mM DSS solution, 100 μL 200 mM phenol and 200 μL D₂O, and then analyzed by ¹H NMR. Because the concentration of the internal standard is known, the liquid product concentration (C) can be determined by the peak area of liquid product.

The Faraday efficiency of liquid product was calculated.

$$FE = \frac{n \times F \times V_l \times C}{Q} \times 100\%$$

(n: transfer electron number; F: Faraday constant; V: Electrolyte volume; C: Molar concentration of liquid product; Q: Total charge.)

The conversion of gas-flow rate of CO₂ to gas-flow rate of gaseous product requires correction coefficient (x_g), which can be obtained by gas chromatography.

The Faraday efficiency of gaseous product was calculated.

$$FE = \frac{x_g \times n \times F \times v \times t \times P / (R \times T)}{Q} \times 100\%$$

(x_g: Product correction factor; n: transfer electron number; F: Faraday constant; v: gas-flow rate; P: standard atmospheric pressure; R: gas constant; T: temperature; Q: Total charge.)

Computational Method:

All the density functional theory calculations were performed by using the Vienna ab initio Simulation Program (VASP).^[1-2] The generalized gradient approximation (GGA) in the Perdew-Burke-Ernzerhof (PBE) form and a cutoff energy of 500 eV for planewave basis set were adopted.^[3] A 3 × 3 × 1 Monkhorst-Pack grid was used for sampling the Brillouin zones at structure optimization.^[4] The ion-electron interactions were described by the projector augmented wave (PAW) method.^[5] The convergence criteria of structure optimization were choose as the maximum force on each atom less than 0.02 eV/Å with an energy change less than 1 × 10⁻⁵ eV. The DFT-D3 semiempirical correction was described via Grimme's scheme method.^[5] The Gibbs free energy change (ΔG) for each elemental step is defined as^[7-8]:

$$\Delta G = \Delta E + \Delta ZPE - T\Delta S + \Delta G_U + \Delta G_{pH} \quad (1)$$

where ΔE and ΔZPE are the adsorption energy based on density functional theory calculations and the zero-point energy correction, respectively. T, ΔS, U, and ΔG_{pH} represent the temperature, the entropy change, the applied electrode potential, and the free energy correction of the pH,

respectively.

***In situ* measurements.**

The *in situ* XAS measurements were conducted at the 1W1B beamline of Beijing Synchrotron Radiation Facility. The *in situ* experiments were carried out in a dedicated *in situ* flow cell. *In situ* XAS measurements were performed at different applied potentials from -0.9 V to -1.2 V versus RHE. The XAS data were analyzed using the software package Athena and Artemis. *In situ* Raman (Horiba Labram HR Evolution Raman System) was conducted using a 785-nm excitation laser in a modified flow cell. *In situ* Raman experiments were performed at different applied potentials from -0.9 V to -1.2 V versus RHE.

The gas electroresponse experiments.

10 mg of the catalysts (Pb/Cu₂O-x and Cu₂O) was evenly dispersed in 1 mL of acetone. Then, 400 μ L dispersion liquid was evenly sprayed on the Ni foam with an exposed area of $1 \times 1 \text{ cm}^{-2}$. After electrically activated, connect the prepared electrode to the two poles of the electrochemical workstation and place it in a closed system filled. The current density was tested at -0.1 V, denoted as j_1 . Subsequently, fill the closed system with CO gas and test the current density at -0.1V, denoted as j_2 . Due to the adsorption of CO on the surface of the catalyst, the current density will change. This difference in current density ($\Delta j = j_2 - j_1$) can reflect the adsorbed capacity of CO on the surface of the catalyst. The higher Δj , the stronger the adsorption of CO on the catalyst.

Supporting Figures

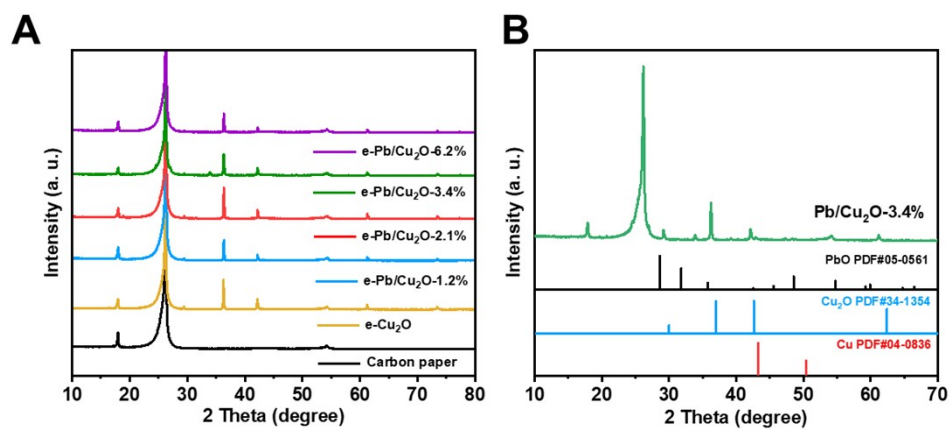


Figure S1. (A) XRD patterns of e-Pb/Cu₂O-x. (B) XRD patterns of e-Pb/Cu₂O-3.4%.

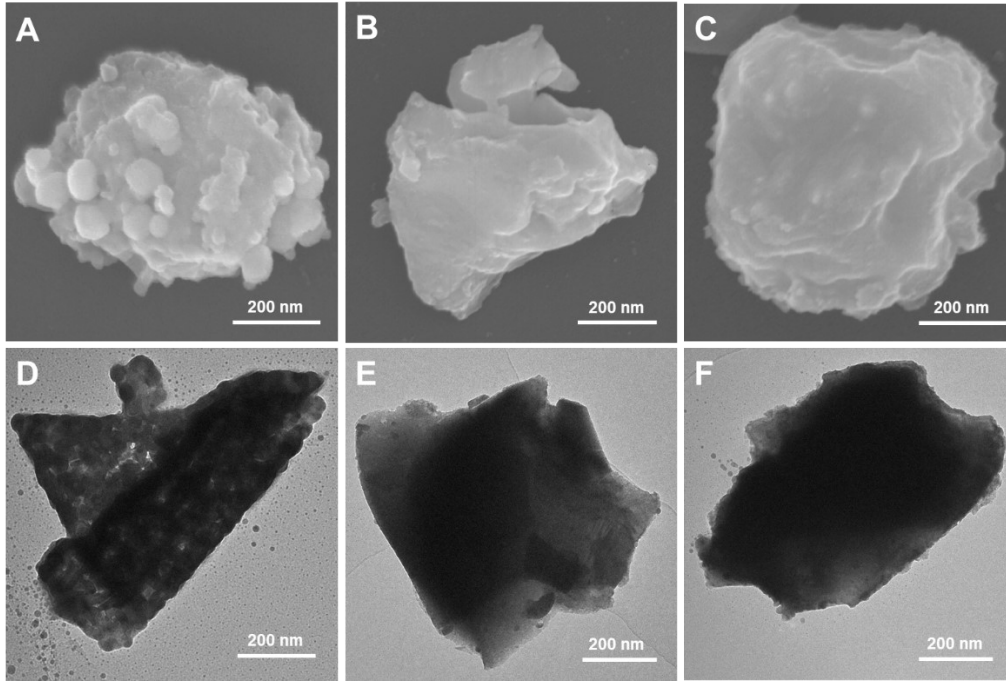


Figure S2. SEM images of (A) e-Pb/Cu₂O-1.2%, (B) e-Pb/Cu₂O-2.1%. (C) e-Pb/Cu₂O-6.2% and TEM images of (D) e-Pb/Cu₂O-1.2%, (E) e-Pb/Cu₂O-2.1%. (F) e-Pb/Cu₂O-6.2%

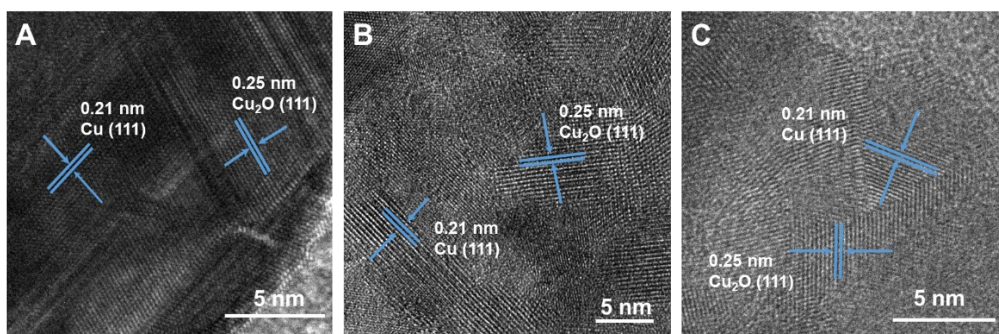


Figure S3. HRTEM images of (A) e-Pb/Cu₂O-1.2%, (B) e-Pb/Cu₂O-2.1%. (C) e-Pb/Cu₂O-6.2%

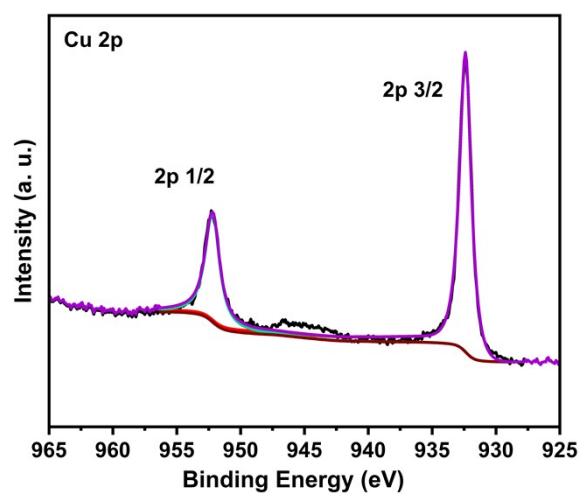


Figure S4. Cu 2p XPS spectra for e-Pb/Cu₂O-3.4%

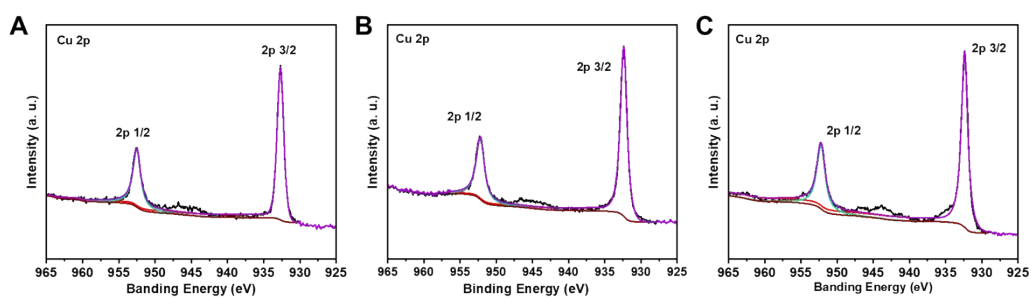


Figure S5. Cu 2p XPS spectra of (A) e-Pb/Cu₂O-1.2%, (B) e-Pb/Cu₂O-2.1%. (C) e-Pb/Cu₂O-6.2%.

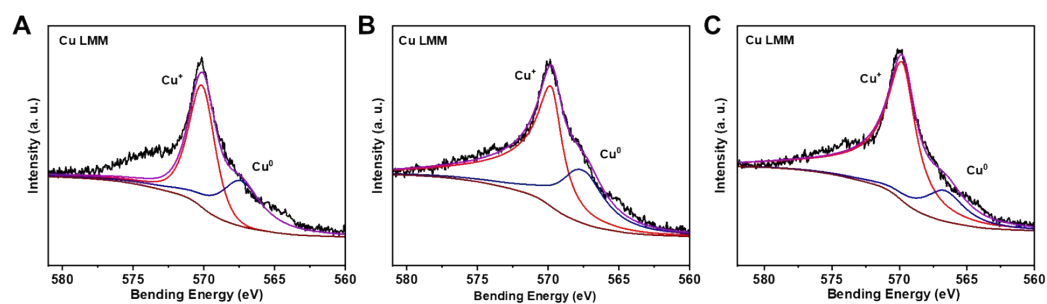


Figure S6. Cu LMM spectra of (A) e-Pb/Cu₂O-1.2%, (B) e-Pb/Cu₂O-2.1%. (C) e-Pb/Cu₂O-6.2%.

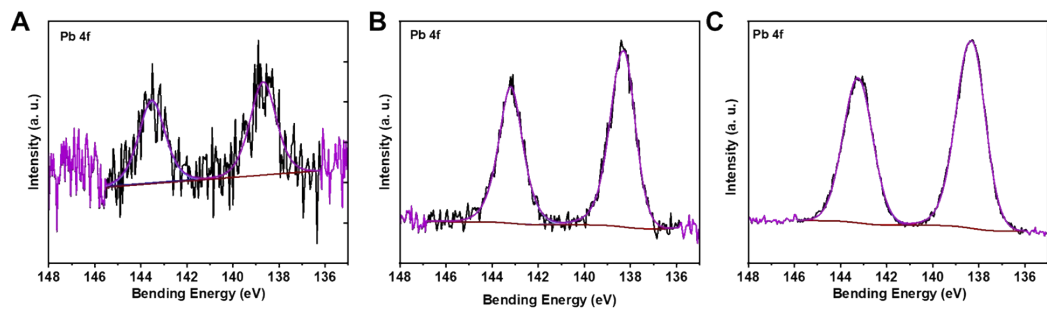


Figure S7. Pb 4f XPS spectra of (A) e-Pb/Cu₂O-1.2%, (B) e-Pb/Cu₂O-2.1%. (C) e-Pb/Cu₂O-6.2%.

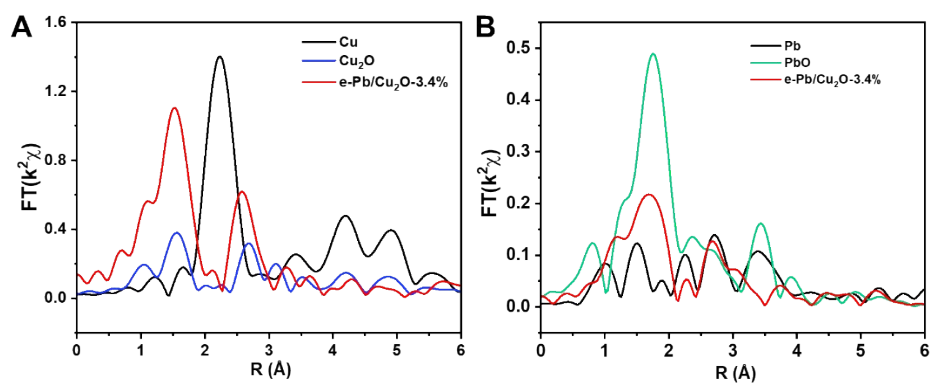


Figure S8. R Spatial data of (A) Cu K-edge EXAFS spectra and (B) Pb L-edge EXAFS spectra for e-Pb/ Cu_2O -3.4%.

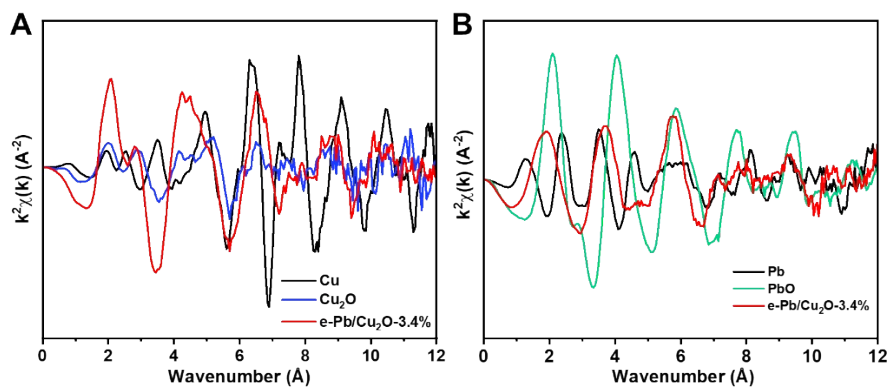


Figure S9. Oscillation function $k^2\chi(k)$ of (A) Cu K-edge EXAFS spectra and (B) Pb L-edge EXAFS spectra for e-Pb/ Cu_2O -3.4%.

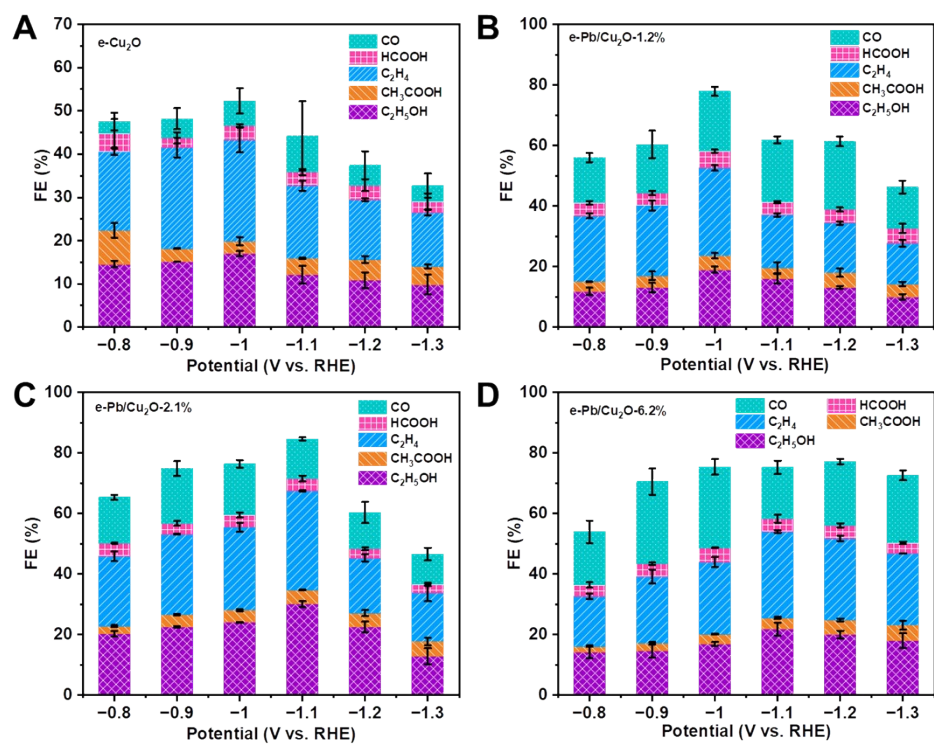


Figure S10. The FE of product at different applied potentials with 10 min electrolysis for (A) e-Cu₂O. (B) e-Pb/Cu₂O-1.2%. (C) e-Pb/Cu₂O-2.1% and (D) e-Pb/Cu₂O-6.2%.

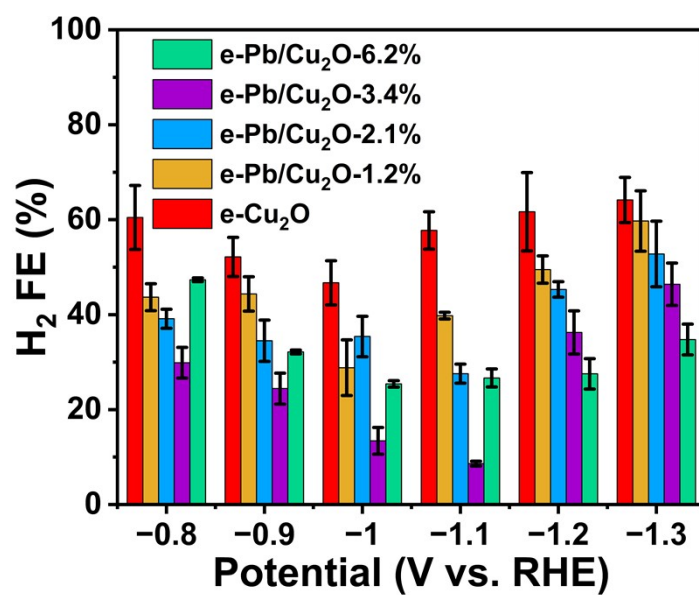


Figure S11. The FE of H₂ at different applied potentials for e-Cu₂O, e-Pb/Cu₂O-1.2%, e-Pb/Cu₂O-2.1%, e-Pb/Cu₂O-3.4% and e-Pb/Cu₂O-6.2%.

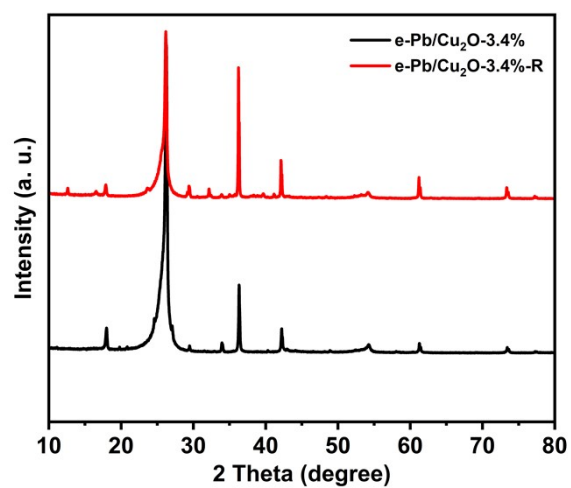


Figure S12. XRD patterns of e-Pb/Cu₂O-3.4% and e-Pb/Cu₂O-3.4%-R.

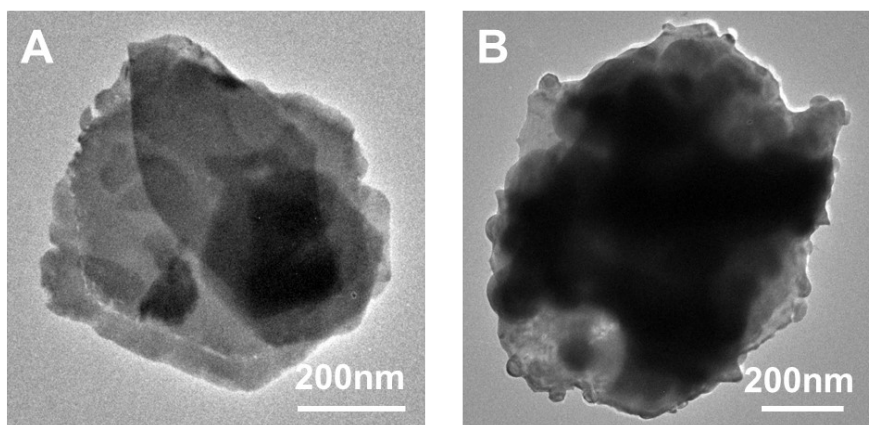


Figure S13. TEM image of (A) e-Pb/Cu₂O-3.4% and (B) e-Pb/Cu₂O-3.4%-R.

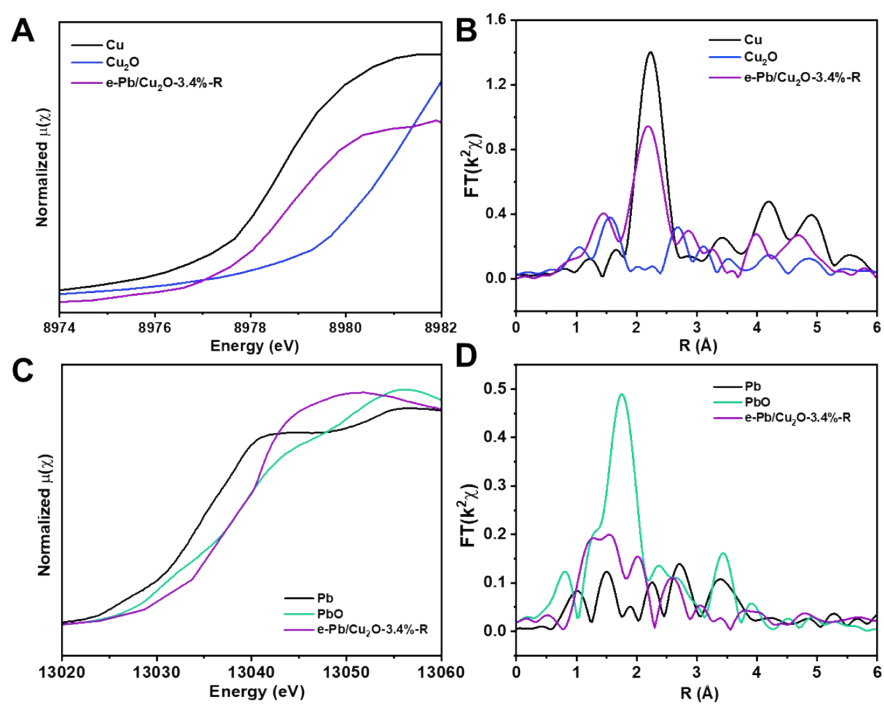


Figure S14. XANES spectra at (A) Cu K-edge and (C) Pb L-edge for e-Pb/ Cu_2O -3.4%-R and R Spatial data of (B) Cu K-edge EXAFS spectra and (D) Pb L-edge EXAFS spectra for e-Pb/ Cu_2O -3.4%-R.

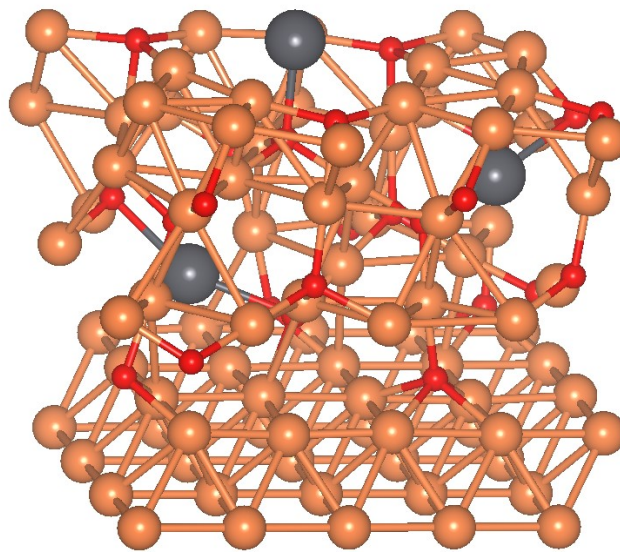


Figure S15. Structural model of Cu(111)-Cu₂O(111)-Pb.

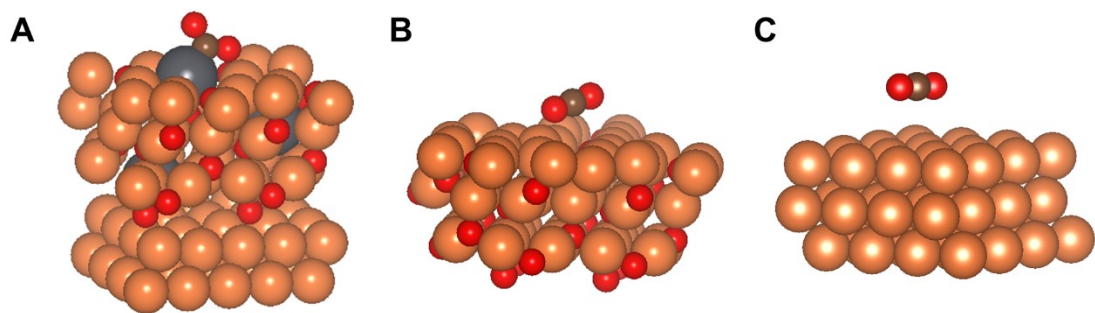


Figure S16. Adsorption of CO₂ on (A) Cu(111)-Cu₂O(111)-Pb; (B) Cu₂O(111) and (C) Cu(111)

Table 1. Comparison of CO₂ reduction performance on different Cu-based catalysts.^[9-23]

Electrode	FE of C ₂ /%	Current density/ mA cm ⁻²	Potential/V	Reference
e-Pb/Cu ₂ O-3.4%	83.9%	203.8	-1.1 V	This work
CuZnO _x	76%	200	-0.99 V	S9
Modified-Cu	>70%	1.1	-1.41 V	S10
SrCuO ₂	53%	>200	-0.83 V	S11
F-Cu	70.4%	400	-1.17 V	S12
AgI-CuO	68.9%	18.2	-1.0 V	S13
Cu ₃ (μ ₃ -OH)(μ ₃ -trz) ₃	80%	14	-0.8 V	S14
Cu ₂ O	74.2%	40	-1.15 V	S15
CuOHfCl	53.8%	15	-1.0 V	S16
Cu	62.8%	2300	-1.94 V	S17
CuBtz	61.6%	938	-1.6 V	S18
CuGa	81.5%	900	-1.07 V	S19
Cu-Ag	80%	<100	-0.56 V	S20
Cu ₃ N _x	81.7%	307	-1.15 V	S21
Cu/N _x C	80%	>20	-1.1 V	S22

Notes and references

- [1] G.Kresse, J. Furthmüller, *Comput. Mater. Sci.* 1996, 1, 15-50.
- [2] G.Kresse, J. Furthmüller, *Phys. Rev. B.* 1996, 16, 11169-11186.
- [3] J.P. Perdew, K. Burke, M. Ernzerhof, *Phys. Rev. Lett.* 1996, 18, 3865-3868.
- [4] H.J. Monkhorst, J.D. Pack, *Phys. Rev. B.* 1976,13, 5188-5192.
- [5] P.E. Blöchl, *Phys. Rev. B.* 1994, 50, 17953-17979.
- [6] S. Grimme, J. Antony, S. Ehrlich and H. Krieg, *J. Chem. Phys.* 2010, 132, 154104.
- [7] J. Rossmeisl, A. Logadottir, J. K. Nørskov, *Chem. Phys.* 2005, 319, 178-184.
- [8] A. A. Peterson, F. Abild-Pedersen, F. Studt, J. Rossmeisl, J. K. Nørskov, *Energy Environ. Sci.* 2010, 3, 1311-1315.
- [9] C. Chang, Y. Lai, Y. Chu, C. Peng, H. Tan, C. Pao, Y. Lin, S. Hung, H. Chen, H. Chen, *J. Am. Chem. Soc.* 2023. doi.org/10.1021/jacs.3c00472.
- [10] W. Nie, G. Heim, N. Watkins, T. Agapie, J. Peters, *Angew. Chem. Int. Ed.* 2023, 62, e202216102.
- [11] X. Lu, B. Lu, H. Li, K. Lim, L. Seitz, *ACS Catal.* 2022, 12, 6663-6671.
- [12] X Yan, C. Chen, Y. Wu, Y. Chen, J. Zhang, R. Feng, J. Zhang, B. Han, *Green Chem.* 2022, 24, 1989-1994.
- [13] R. Yang, J. Duan, P. Dong, Q. Wen, M. Wu, Y. Liu, Y. Liu, H. Li, T. Zhai, *Angew. Chem. Int. Ed.* 2022, 61, e202116706.
- [14] D. Huang, H. Zhu, Z. Zhao, J. Huang, P. Liao, X. Chen, *ACS Catal.* 2022, 12, 8444-8450.
- [15] Y. Jiang, X. Wang, D. Duan, C. He, J. Ma, W. Zhang, H. Liu, R. Long, Z. Li, T. Kong, X. Loh, L. Song, E. Ye, Y. Xiong, *Adv. Sci.* 2022, 9, 2105292.
- [16] M. Li, Y. Ma, J. Chen, R. Lawrence, W. Luo, M. Sacchi, W. Jiang, J. Yang, *Angew. Chem. Int. Ed.* 2021, 60, 11487-11493.
- [17] C. Zhu, Y. Song, X. Dong, G. Li, A. Chen, W. Chen, G. Wu, S. Li, W. Wei, Y. Sun, *Energy Environ. Sci.* 2022, 15, 5391-5404.
- [18] H. Zhu, H. Chen, Y. Han, Z. Zhao, P. Liao, X. Chen, *J. Am. Chem. Soc.* 2022, 144, 13319-13326.
- [19] P. Li, J. Bi, J. Liu, Y. Wang, X. Kang, X. Sun, J. Zhang, Z. Liu, Q. Zhu, B. Han, *J. Am. Chem. Soc.* 2023, 145, 4675-4682.

- [20] J. Li, H. Xiong, X. Liu, D. Wu, D. Su, B. Xu, Q. Lu, *Nat. Commun.* 2023, 14, 698.
- [21] C. Peng, G. Luo, Z. Xu, S. Yan, J. Zhang, M. Chen, L. Qian, W. Wei, Q. Han G. Zheng, *Adv. Mater.* 2021, 33, 2103150.
- [22] Z. Li, Y. Yang, Z. Yin, X. Wei, H. Peng, K. Lyu, F. Wei, L. Xiao, G. Wang, H. Abruña, J. Lu, L. Zhuang, *ACS Catal.* 2021, 11, 2473-2482.